ISSN 1674-1056
http://cpb.iphy.ac.cn
http://iopscience.iop.org/cpb
中国物理 B
Chinese Physics
中国物理 Chinese Physics B

Tunable inhibition of *β*-amyloid peptides by fast green molecules

Tiantian Yang(杨甜甜), Tianxiang Yu(俞天翔), Wenhui Zhao(赵文辉), and Dongdong Lin(林冬冬)
Citation: Chin. Phys. B, 2021, 30 (**8**): 088701. DOI: 10.1088/1674-1056/ac0690
Journal homepage: http://cpb.iphy.ac.cn; http://iopscience.iop.org/cpb

What follows is a list of articles you may be interested in

Structural and dynamical mechanisms of a naturally occurring variant of the human prion protein in preventing prion conversion

Yiming Tang(唐一鸣), Yifei Yao(姚逸飞), and Guanghong Wei(韦广红)†
Chin. Phys. B, 2020, 29 (**10**): 108710. DOI: 10.1088/1674-1056/aba9ba

Electron beam irradiation on novel coronavirus (COVID-19): A Monte-Carlo simulation

Guobao Feng(封国宝), Lu Liu(刘璐), Wanzhao Cui(崔万照), Fang Wang(王芳)
Chin. Phys. B, 2020, 29 (**4**): 048703. DOI: 10.1088/1674-1056/ab7dac

Probing conformational change of T7 RNA polymerase and DNA complex by solid-state nanopores

Xin Tong(童鑫), Rui Hu(胡蕊), Xiaoqing Li(李晓晴), Qing Zhao(赵清)
Chin. Phys. B, 2018, 27 (**11**): 118705. DOI: 10.1088/1674-1056/27/11/118705

Individual identification using multi-metric of DTI in Alzheimer's disease and mild cognitive impairment

Ying-Teng Zhang(张应腾), Shen-Quan Liu(刘深泉)
Chin. Phys. B, 2018, 27 (**8**): 088702. DOI: 10.1088/1674-1056/27/8/088702

Amyloid-*β* peptide aggregation and the influence of carbon nanoparticles

Wen-Hui Xi(郗文辉) and Guang-Hong Wei(韦广红)
Chin. Phys. B, 2016, 25 (**1**): 018704. DOI: 10.1088/1674-1056/25/1/018704

Tunable inhibition of β-amyloid peptides by fast green molecules*

Tiantian Yang(杨甜甜)[1], Tianxiang Yu(俞天翔)[1], Wenhui Zhao(赵文辉)[1,†], and Dongdong Lin(林冬冬)[1,2,‡]

[1] *Department of Microelectronic Science and Engineering, Department of Physics, School of Physical Science and Technology, Ningbo University, Ningbo* 315211, *China*

[2] *Qian Xuesen Collaborative Research Center of Astrochemistry and Space Life Sciences, Ningbo University, Ningbo* 315211, *China*

(Received 15 May 2021; revised manuscript received 26 May 2021; accepted manuscript online 29 May 2021)

The aggregation of β-amyloid (Aβ) protein into toxic intermediates and mature fibrils is considered to be one of the main causes of Alzheimer's disease (AD). Small molecules as one of blockers are expected to be the potential drug treatment for the disease. However, the nucleation process in molecular assembly is less informative in the literatures. In this work, the formation of Aβ(16-22) peptides was investigated with the presence of small molecule of fast green (FG) at the initial aggregation stage. The results exhibited the tunable inhibitory ability of FG molecules on Aβ(16-22) peptides. Atomic force microscopy (AFM) demonstrated that the inhibitory effect would be dependent on the dose of FG molecules, which could delay the lag time (nucleation) and form single layer conjugates. Spectral measurements further showed that the β-sheet secondary structure of Aβ(16-22) reduced dramatically after the presence of FG molecules. Instead, non-β-sheet nanosheets were formed when the FG/Aβ(16-22) ratio reached 1:1. In addition, the cytotoxicity of aggregates reduced greatly with the presence of FG molecules compared with the Aβ(16-22) fibrils. Overall, this study provided a method for suppressing the toxic amyloid aggregates by FG molecules efficiently, and also showed a strategy for fabrication of two-dimensional materials by small molecules.

Keywords: amyloid, fast green, aggregation, Alzheimer's disease

PACS: 87.15.–v, 87.14.E–, 31.15.xv, 68.37.Ps **DOI:** 10.1088/1674-1056/ac0690

1. Introduction

Alzheimer's disease (AD) is one of the commonest types of dementia related with the neurodegenerative diseases.[1–3] The main clinical manifestation of AD is the formation of brain plaques due to protein misfolding. AD's pathological features are usually considered to be the accumulation of β-amyloid protein in the cerebral cortex/hippocampus and the intracellular hyperphosphorylated tau protein neurofibrillary tangled deposits.[4–6] Specifically, β-amyloid is composed of amyloid precursor protein (APP) that hydrolyzed by two secretases, β- and γ-, with a total length of 39–42 amino acid.[7,8] Additionally, most of the researches show that Aβ from non-toxi monomers undergo conformational changes and self-assembled into toxic intermediates.[9,10] As a result, how to prevent the formation and dissociation of the toxic aggregates is becoming increasingly significant for the therapy of related diseases.

Aβ(16-22) is a short peptide chain composed of seven amino acid residues, Lys-Leu-Val-Phe-Phe-Ala-Glu (KLVFFAE, Fig. 1(a)). This fragment, as one of the shortest chains forming amyloid fibrils, contains key central hydrophobic cluster, which is of importance for the aggregation of β peptides into amyloid fibrils.[11,12] As a result, Aβ(16-22) peptides were investigated extensively by experiments and simulations as the typical amyloid research model. Solid-state nuclear magnetic resonance (NMR) found that Aβ(16-22) would form antiparallel β-sheet strcture under the action of hydrophobic residue.[13] In addition, accumulation and interaction of side chain between peptides, play an important role in determining the fibrils structure.[14] On the other hand, amyloid formed by proteins has a uniform "cross-β" structure stacking repetitively into long fibrils with favorable chemical and mechanical properties. They exhibit favorable features including thermal stability and high bending rigidty, tunable self-assembly, homogenous fabricating and integration of functionality, and high-yield rate by bio-synthesis. These excellent properties promote the extensive exploitation of amyloid fibrosis as a kind of potential bio-nanomaterial. For instance, previous studies found that Italian mutation of Aβ(16-22) (KLVFFAK) could self-assemble into 2D nanosheet with a width of $\sim$ 200 nm, far larger than typical fibrils peptides (3–10 nm).[15] The peptides (YSATFTY) incubated with freshly cleaved MoS_2 substrates can assemble into elongated islands aligned along three equivalent directions on MoS_2 (0001).[16]

To inhibit or accelerate the aggregation of β-amyloid and reduce the cytotoxicity, carbon nanomaterials (nanotube,[17,18] fullerene,[19] dots,[20,21] etc.) and small molecules (EGCG,[22] heparin,[23] 8-bis (2,4-dihydroxyphenyl)-7-hydroxyphenoxazin-3-one,[24,25] etc.) were investigated extensively and exhibited good functions. Triarylmethane dyes, such as acid fuchsin sulfonated triphenyl methane derivative

*Project supported by the National Natural Science Foundation of China (Grand No. 11804174), Qian Xuesen Collaborative Research Center of Astrochemistry and Space Life Sciences, and K. C. Wong Magna Fund in Ningbo University.

†Corresponding author. E-mail: zhaowenhui@nbu.edu.cn

‡Corresponding author. E-mail: lindongdong@nbu.edu.cn

© 2021 Chinese Physical Society and IOP Publishing Ltd

acid fuchsin, have an inhibitory effect on human islet amyloid peptides (hIAPP).[26] There are also some edible pigments that have the same inhibitory effect, such as Curcumin,[27] Methylene blue,[28] Congo red,[29] and so on. Self-assembly is described by the concepts named nucleated conformational conversion mechanism with the oligomers serving as a precursor of amyloid nucleation and converting to amyloid nuclei under certain concentration and interpeptide interactions. As a result, the state of nucleation has a fatal influence to the self-assembly process. Based on the previous studies, we found the small molecule named fast green (FG, Fig. 1(b)) exhibited better manipulation ability for the aggregation of Aβ(16-22) fragments. FG is a biocompatible triarylmethane food dye, with the molecular formula of $C_{37}H_{34}N_2O_{10}S_3Na_2$. Previous studies have shown that FG molecules could suppress the generation of lysozyme fibrils in a concentration-dependent manner, as well as disaggregating activity against the preformed lysozyme fibrils.[30] Furthermore, FG molecules act as a positive inhibitor of hIAPP fibril that binds to the 2^+ and 3^+ monomeric charge states of hIAPP.[31] Recently, studies showed that FG molecules could inhibit Aβ fibrillogenesis, disintegrate mature fibrils, reduce the cytotoxicity, and attenuate Aβ-induced cognitive impairment in mice.[32] Their AFM and ThT fluorescence results demonstrated the great suppression effects by FG molecules. However, the interaction between peptides and FG molecules remains to be explored, especially for the details of nucleation at the initial stage.

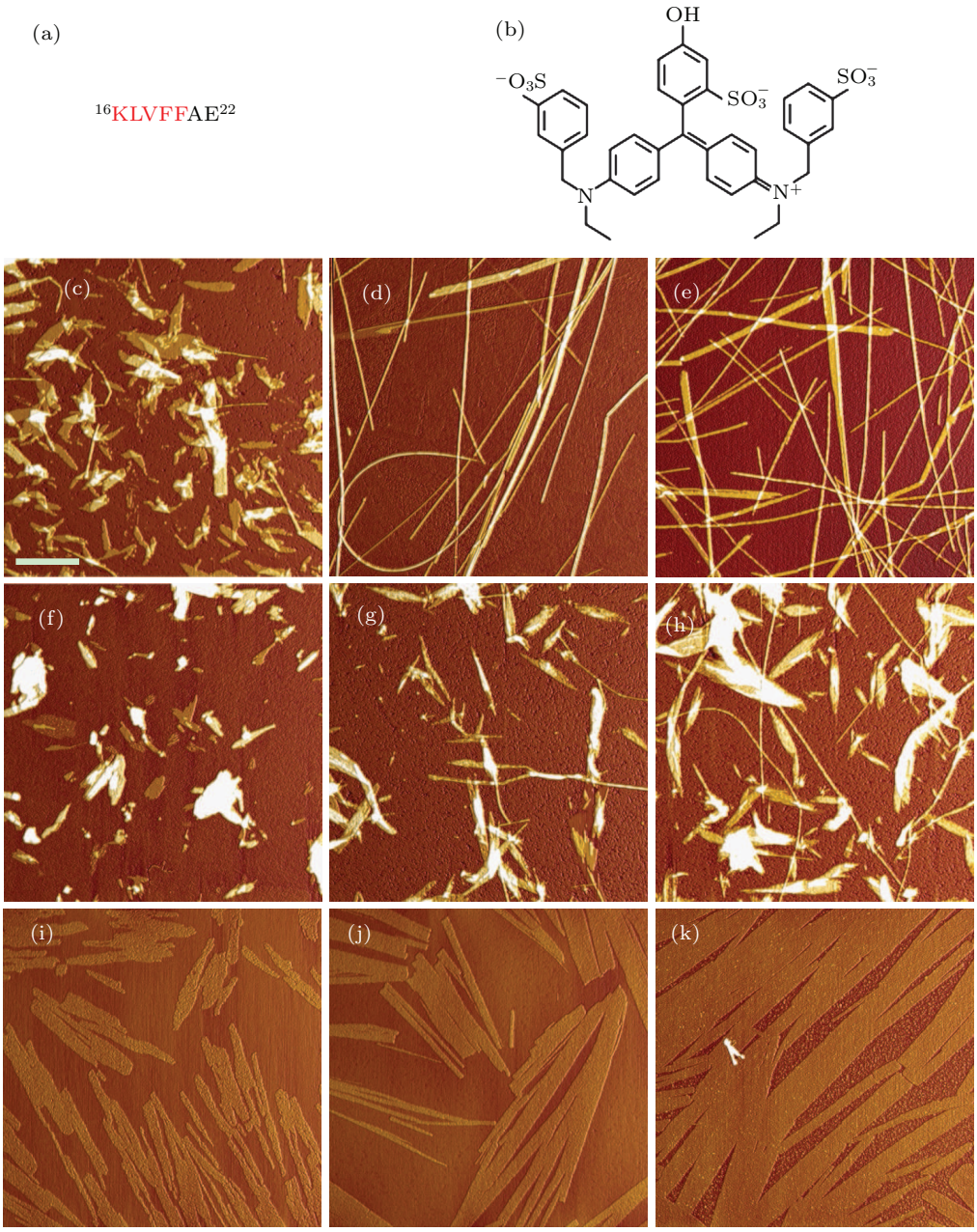


Fig. 1. (a) Aβ(16-22) peptide; (b) FG molecule; (c)–(k) *ex situ.* AFM topography of Aβ(16-22), Aβ(16-22)-FG after incubating at 37 °C for three time points: (c), (f), (i) freshly prepared (30 min); (d), (g), (j) 5 h; (e), (h), (k) 24 h. AFM images of (c)–(e) represent Aβ(16-22) without FG molecules, (f)–(h) represent Aβ(16-22):FG=2:1, while AFM images of (i)–(k) have concentration ratio of 1:1. Scale size: 5.0×5.0 μm^2.

In this work, the inhibitory effect of the FG on amyloid was explored by atomic force microscopy (AFM) and spectral methodology, combined with molecular dynamic simulation (MD). AFM morphology and force measurements were applied to investigate the strong inhibitory ability to the aggregation of Aβ(16-22) fragments by FG molecules with different concentrations. The morphology transformation in the lag phase time was explored in detail. Moreover, Fourier transform infrared spectroscopy (FTIR) and circular dichroism spectra (CD) were measured to explore the β-sheet secondary structure of Aβ(16-22) with different concentration of FG molecules. Furthermore, molecular dynamics simulation was also performed to investigate the molecular interaction between Aβ(16-22) peptides and FG molecules.

2. Results and discussion

2.1. FG molecules prevent the formation of amyloid fibrils with a concentration dependent manner

To examine the inhibitory effect of FG molecules on the Aβ(16-22) peptides, the kinetics and morphological changes of Aβ(16-22) peptides in the presence and absence of FG molecules were measured by AFM at different co-incubation periods. As shown in Figs. 1(c)–1(e), similarly with our previous results,[33] flake aggregates were found immediately after the co-incubation of Aβ(16-22) peptides (40 μM, 30 min). The results keep in line with a variety of studies that the KLVFF (residue 16-20) segment is the most amyloid-prone portion of Aβ peptides, and responsible for initial aggregation and nucleation.[34] As shown in Fig. 1(d), fibrils were quickly formed in 5 h, while abundant mature fibrils self-assembled after 24 h (Fig. 1(e)). Then the fibrils kept in irreversible formation for a long time (month level). Interestingly, the number of flakes reduced ($\sim$ 68% decrement, Fig. S1) when the FG molecules (20 μM) were presented in Aβ(16-22) peptides (Fig. 1(f)). Similar results were found in 5 h (Fig. 1(g)) and 24 h (Fig. 1(h)) checking points. Only few fibrils were formed compared with Aβ(16-22) peptides that without FG molecules. In addition, the flakes kept steady even in 24 h. We owned this phenomenon to the delaying of lag time by FG molecules which could strengthen the intermolecular stacking between Aβ(16-22) peptides. Surprisingly, full of large area flakes were found on the mica substrate when the ratio of the concentration reached to 1:1 (40 μM of Aβ(16-22) and 40 μM of FG molecules), without any fibrils being formed in the whole aggregation process. The results indicated that the FG molecules totally inhibited the amyloidogenesis in the peptide/FG ratio of 1:1 (Figs. 1(i)–1(k)).

Further analysis was made to investigate the topologically changes after the presence of FG molecules. Figures 2(a), 2(d), an 2(g) are the AFM images when the ratio of concentration of peptides/FG is 1:0, 2:1, and 1:1, respectively. Figures 2(b), 2(e), and 2(h)) are the height profiles corresponding to the AFM images, respectively (three white dash lines in different positions of the substrates). Figures 2(c), 2(f), and 2(i) show the height distributions (with Gauss fit) from 5 different AFM images in the initial state (30 min). Flat and homogeneous small flakes were found in Aβ(16-22) solution which had no FG molecules in the beginning. All of the thin flakes with a height of approximately 2.4 nm could be clearly measured in Fig. 2(a). In addition, flakes with a thickness of 5 nm were also found in the same sample, which indicated that the double layer flakes would be one of the intermediates in the aggregation process (Fig. 2(b)). According to the previous studies, 2.4 nm scale was considered to be orderly assembled from a seven residues peptide in its longitudinal direction.[35,36] As a result, we speculated that the flakes with 2.4 nm thickness were in single peptide layer. Height distribution observed from 5 different AFM images confirmed that most of the flakes were in single and double layers, or even in triple layers (Fig. 2(c)). However, the majority of morphology changed when the FG molecules were co-incubated with the concentration ratio of 2:1. Except with the single and double layer flakes, large scale aggregates were formed with the height varying from $\sim$ 3 nm to 19 nm (Figs. 2(d)–2(f)), indicating the binding of FG molecules. When the concentration ratio increased to 1:1, a new type of flakes was formed, with an extremely small height of $<$ 1 nm (Figs. 2(g)–2(i)). Furthermore, the new flakes grew large with the incubation time going on (Figs. 2(g)–2(i)). However, there was no large increase in the thickness of the flakes. All of the flakes kept at $\sim$ 0.9 nm from beginning to 24 h (Fig. S2). Those thin layers were firstly measured when the Aβ(16-22) peptides were co-incubated with FG molecules at the ratio of 1:1. To exclude the possibility that those flakes were not FG molecules aggregates, pristine FG molecules solution (4, 40, and 400 μM) were measured by AFM (Fig. S3). The result revealed that only two types of tiny particles were formed, which were totally different from the morphology of flakes.

The mechanical properties of those special aggregates were explored by AFM. Here, adhesion forces were obtained by measuring the degree of distortion in a cantilever on the surface of the sample.[37,38] In nitrogen gas condition, the adhesion force typically consists of van der Waals force and electrostatic force. In Fig. 3, the flakes from Aβ(16-22) peptides and nanosheets from mixed solution (the concentration ratio of peptides/FG molecules was 1:1) were selected. The adhesion force of mica surface from the two samples was controlled at $\sim$ 17.5 nN. It can be seen that the nanosheets have a lower adhesion force than that of the flakes ($\sim$ 14.7 nN and $\sim$ 15.6 nN on average, respectively). The difference of adhesion force gave strong evidence that those nanosheets were not constructed by pure peptides but Aβ(16-22) and FG molecules conjugates. In addition, the high adhesion force of flakes further indicated that the charged residues were inclined to exposed on the surface,[39] which gave evidence of the assembly of flakes in longitudinal direction. Besides, it also revealed that FG molecules potentially prevent a direct peptide/peptide interaction, and promote a strong peptide/FG molecule interaction.

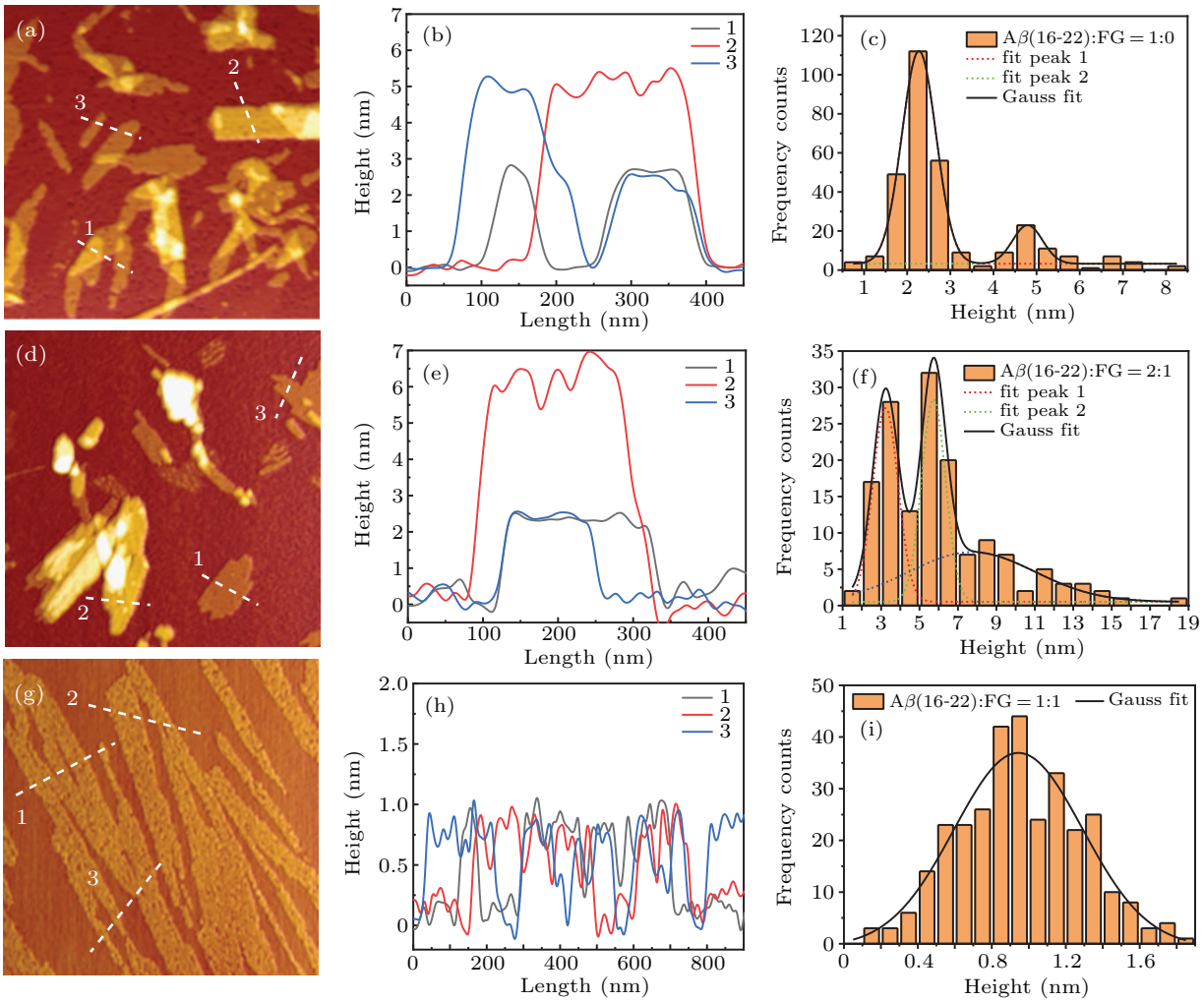


Fig. 2. Zoom in AFM images and their height profiles form initial state (30 min). (a), (d), (g) AFM images of different peptides/FG concentration ratio (1:0, 2:1, 1:1, respectively). (b), (e), (h) Height profiles corresponding to AFM images, respectively (three white dash lines in different positions of substrates). (c), (f), (i) Height distribution (with Gauss fit) from 5 AFM images in initial state (30 min), respectively.

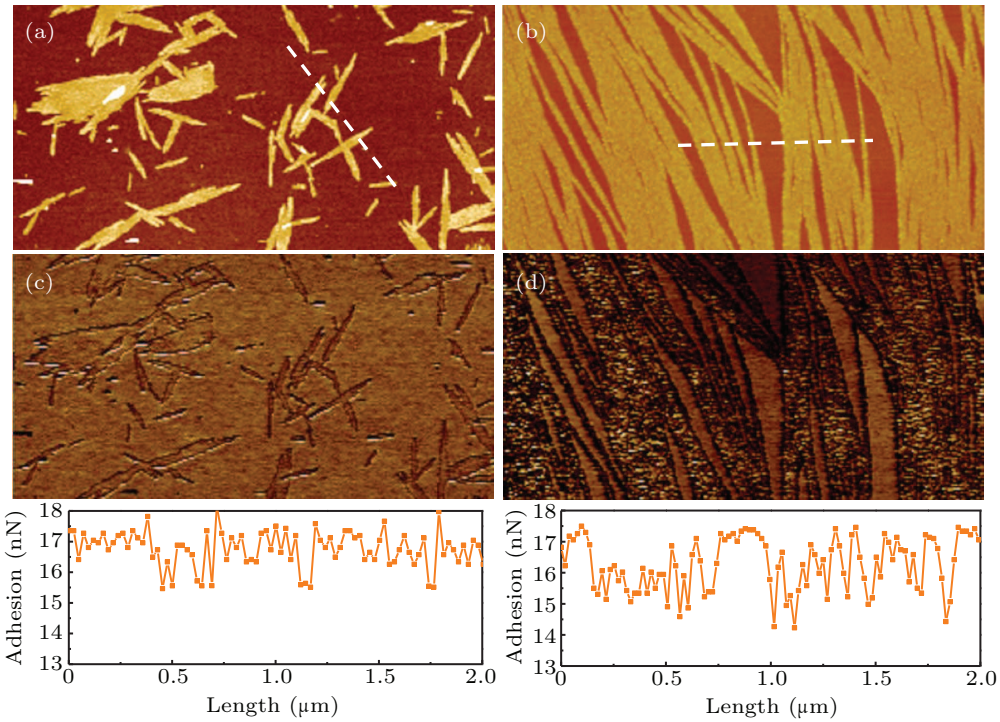


Fig. 3. Measurements of adhesion force by AFM. (a) AFM topological image of Aβ(16-22) flakes. (b) AFM topological image of nanosheets of Aβ(16-22)/FG concentration ratio of 1:1. (c), (d) AFM adhesion map of Aβ(16-22) flakes and nanosheets, respectively.

2.2. FG molecules reduce the β-sheet secondary dramatically

In order to explore the structural transformation with the presence of FG molecules, spectra methods were applied. Vibrational spectroscopy (FTIR) technique is one of the mature and well established experimental techniques for the analysis of secondary structure of proteins and polypeptides, which is convenient, label free, and can be used under a wide variety of conditions.[40,41] Here, the peptides/FG molecules concentration ratios of 0:1, 4:1, 2:1 and 1:1 were prepared and measured by FTIR, as shown in Fig. 4(a). The most sensitive spectral region to the protein secondary structural components is the amide I band (1700–1600 cm^{-1}), which is due to the C=O stretch vibrations of peptides.[41] The pure Aβ(16-22) peptides can easily aggregate into fibrils, occupying the largest intensity at $\sim$ 1625 cm^{-1}.[40] With the FG molecules gradually presented into solution at different ratios, it can be found that the peak located at $\sim$ 1625 cm^{-1} decreased accordingly. When the ratio reached 1:1, only tiny peak could be found, indicating the significant decrease of β-sheet structures. In addition, the spectrum of FG molecules was also measured (Fig. 4(a), purple curve). Typical band at $\sim$ 1550 cm^{-1} represents the CN stretching and NH bending of molecule.

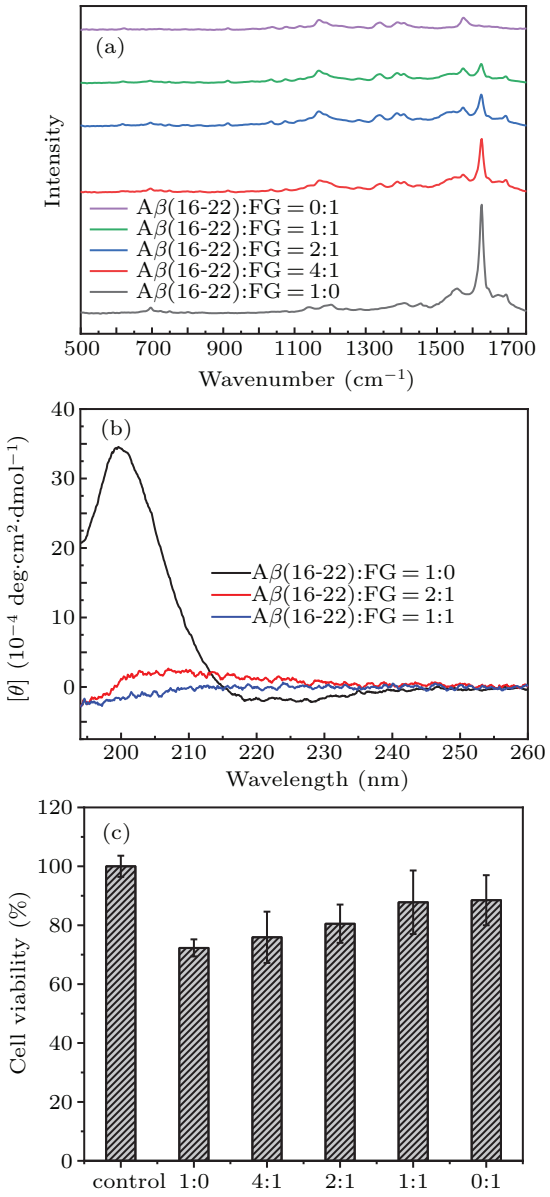


Fig. 4. (a) FTIR spectra of ratio dependence, Aβ(16-22)/FG concentration ratios are 1:0, 4:1, 2:1, 1:1, 0:1, respectively. (b) CD spectra, Aβ(16-22)/FG concentration ratios are 1:0, 2:1, 1:1, respectively. (c) Cell viability of FG molecules, Aβ(16-22) peptides, Aβ(16-22) peptides with FG molecules incubated for 24 hours, respectively. The values were normalized by control sample each time. From left to right: control, Aβ(16-22)/FG concentration ratios of 1:0, 4:1, 2:1, 1:1, 0:1, respectively.

CD spectra further proved our results by measuring three typical concentration ratios of 1:0, 2:1 and 1:1. As shown in Fig. 4(b), the typical β-sheet secondary structure of Aβ(16-22) peptides was clearly observed in CD spectra (positive peak at $\sim$ 198 nm and negative peak at $\sim$ 220 nm).[42] It was noteworthy that the intensity of CD signal representing β-sheet secondary structure decreased with the ratio of FG molecules increasing from 0 to 40 μM. As a result, the FTIR and CD results suggested that less amyloid peptides assembly with β-sheet secondary structures formed upon interference with FG molecules. These results were also in accordance with our AFM observation well.

2.3. The conjugates of FG molecules and peptides increase the cell viability

Another problem could be focused on the cytotoxicity of those peptide/FG conjugates. FG molecules were believed to bind with the monomers and early formed oligomers. The conjugates inhibit the further fibrillation, and are expected to promote the transformation of toxic intermediates to "off-pathway" nontoxic oligomeric isoforms. Due to the biocompatible property of FG molecules, the results (Fig. 4(c)) demonstrated that those flakes had low cytotoxicity compared with pure Aβ(16-22) fibrils, which obtained a cell viability of $\sim$ 72.3% (1:0, fibrils were already formed in 24 h). Additionally, the high ratio of FG molecules reduced more toxic aggregates, leading to a better cell viability when the concentration ratio reached to 1:1. As a result, the cell viability results confirmed that FG, a type of food dye, could be nontoxic for the related drug design.

2.4. PHE, LYS, and LEU have a tight interaction with FG molecules

Finally, a brief MD simulation was performed to explore the inhibitory effect by FG molecules. As shown in Figs. 5(a)–5(d), Aβ(16-22) peptides in the absence/presence of FG molecules were investigated. Six random Aβ(16-22) monomer were designed at the initial state. The β-sheet structures were well established after a 600 ns simulation of Aβ(16-22) peptides, which is well in line with the previous results.[19] When the FG molecules were presented in the sys-

tem (the concentration ratio: 2:1), strong suppression ability could be found that only one pair of β-sheet structure was formed, as they have no contact with FG molecules in 600 ns (Figs. 5(c)–5(e)). The snapshots of interaction process at 50 ns, 100 ns, 200 ns, and 400 ns were also shown in Fig. S4. The strong binding of FG molecule to peptides was observed at early 50 ns simulation, preventing the formation of β-sheet structures. To explore the interaction details, minimum distance was further calculated as shown in Fig. 5(f).[43] Residues of PHE, LYS, and LEU have a tight interaction with FG molecules. The electrostatic interaction and π–π interaction between aromatic ring and F20 strengthen the stability of peptides/FG conjugates, keeping them separately in the solution to avoid the fibrillogenesis. Furthermore, compared with our AFM observation, we believed that the large thin flakes would be the rearrangement of peptides/FG conjugates driven by the flat mica surface. The crystal orientation of mica promotes the peptides and FG molecules lying on the surface.[16]

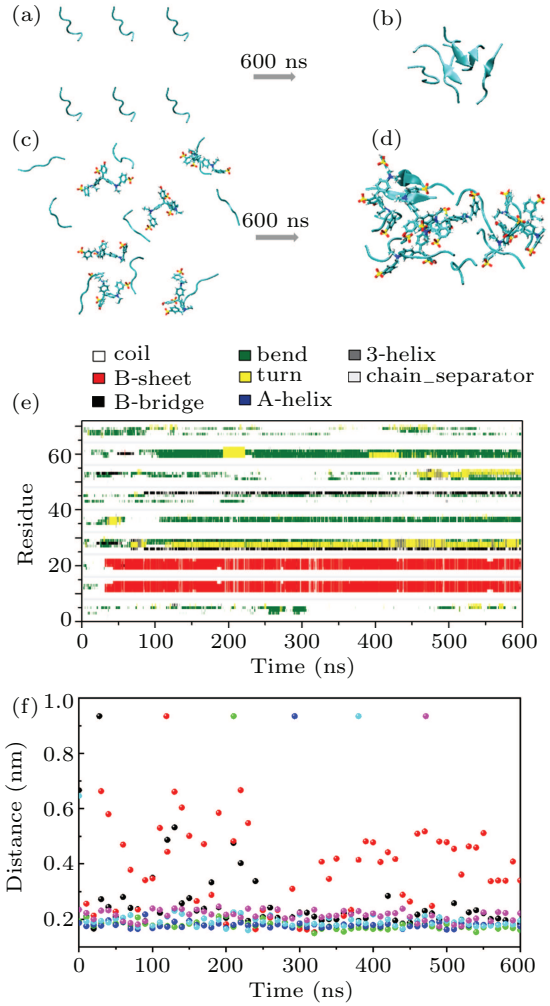


Fig. 5. MD simulation of aggregation process by free Aβ(16-22) peptides and Aβ(16-22) peptides with FG molecules (ratio of 2:1). (a) Six random structure Aβ(16-22) peptides at initial state. (b) Aβ(16-22) fibrils after 600 ns simulation. (c) Aβ(16-22) peptides with FG molecules (ratio:2:1) at initial state. (d) Aβ(16-22) peptides with FG molecules (ratio of 2:1) conjugates after 600 ns simulation, together with its secondary structure map (e). (f) Distribution of minimum distance of each residue as a function of time (0–600 ns).

3. Conclusions

The inhibitory effect and fabrication of two-dimensional material by FG (a type of food dye) were systemically investigated by experiments and MD simulations. AFM, CD, and FTIR measurements revealed the dose dependent manner of suppression effect by FG molecules. The results demonstrated that FG molecules could delay the nucleation of oligomers and make structural transformation of single layer of flakes. The inhibitory ability reached the largest when the ratio of concentration of peptide/FG increased to 1:1, together with ordered and stable nanosheets being formed. In addition, both FTIR and CD spectra exhibited dramatic decrease of β-sheet structures. The adhesion force measurements further exhibited that the nanosheets were conjugates with low adhesion force. Based on our MD simulation, inhibitory phenomenon (strong interaction with PHE, LYS, and LEU) was also clearly observed in a 600 ns simulation at 310 K. Finally, cell viability results revealed that the biocompatible FG molecules have less toxicity in any peptide/FG ratio, which can be potentially developed as a potential anti-AD drug. With the control of peptide/FG ration, the formation of thin layer of flakes and nanosheets on mica substrate may also be a cheap strategy to build bio-functional materials.

4. Material and methods

4.1. Materials

Synthetic Aβ(16-22) was purchased from GL biochem Ltd. (Shanghai, China).[44] The final purity reaches about 98%. Fast green (FG, purity $\geq$ 98.0%), cytotoxicity assay kit (WST-1), PBS powder, and dulbecco modified eagle medium (DMEM) were purchased from Sigma-Aldrich (Shanghai) Ltd. The FG was added in Aβ(16-22) solution directly with the set values, assisted by gentle ultrasonic apparatus. SH-SY5Y cells were purchased from Fudan IBS Cell Center. All of the deionized water used in this study was made by a Millipore purification system with a minimum resistivity of 18.2 MΩ·cm.

Aβ(16-22) solution was prepared by adding 14.654 mL of deionized water to 1 mg of Aβ(16-22) dry powder (the storage condition of the dry powder is -20 °C). Then the dry powder was diluted to 80 μM, and shook for 30 s. The spare centrifuge tubes were used to store 200 μL of Aβ(16-22) solution and sook with a oscillator for 30 s. The final concentrations of Aβ(16-22) in the four centrifuge tubes were 40 μM, 20 μM, 10 μM, and 0 μM, respectively.

4.2. Atomic force microscopy

The experimental solution was prepared with the concentration ratio of 1:0, 1:1, 2:1, 4:1, and 0:1 respectively. Clean and flat mica pieces with a cut size of 8 mm × 8 mm were pasted on the round iron pieces with a diameter of about

12 mm by double-sided adhesive tape. Then the upper mica pieces were stripped to obtain a clean mica layer before use. After shaking the freshly prepared solution for 30 s, 5 μL of the freshly solution of various concentrations were dropped on the mica slice, dried naturally at room temperature, and then placed in AFM (Multimode VIII, Bruker Nano Surface, USA)) to observe the morphology. The remaining solution in the centrifuge tube was placed in a metal bath with a constant temperature of 37 °C. Tapping mode was applied in the air, with the resonant frequency of 1.0 Hz. The obtained AFM images were processed by NanoScope Analysis.

4.3. Fourier transform infrared spectroscopy

Fourier transform infrared spectroscopy (FTIR, Cary660, Agilent) was applied to study the secondary structure of peptides and proteins. 5 μL of the freshly prepared solution of various concentrations were dropped on the platform and dried quickly with nitrogen gas. The infrared spectrum was tested under the mode and parameters set by the software. Before scanning the sample signal, it is necessary to scan the background signal of the empty optical path. After subtracting the background, the computer performed Fourier transform to obtain the infrared spectrum of the sample.

4.4. Cell viability experiment

WST-1 assay was used to perform cell viability experiments.[45] Before experimenting, SH-SY5Y cells were placed in DMEM medium (10% fetal bovine serum (FBS), 100 units/mL penicillin (1%), 100 μg/mL streptomycin (10%)) in a humid environment at 37 °C (95% air, 5% CO_2). During the experiment, the DMEM supplemented with 10% FBS was replaced with a medium containing 1% FBS. Subsequently, the cell culture medium was transferred to a 96-microwell plate. A volume of 100 mL was dropped into each well, and incubated for 24 h. Finally, 10 μL WST-1 solution (5 mg/mL) was added into samples for another incubation of 2 h. All of the samples were measured at 450 nm and calculated by comparing the optical densities (O.D) value from each well with that of untreated SH-SY5Y cells in the same condition. All results were exhibited with the mean ± SE standard error from 5 wells in each group.

4.5. MD simulation

The initial structure of FG molecule was obtained from the Pubchem library (https://pubchem.ncbi.nlm.nih.gov). The parameters for van der Waals and bonded interactions were obtained from the Amber force field, and the parameters for electrostatic interactions were obtained by fitting quantum mechanical calculated potentials. All of the MD simulations were performed by using the GROMACS-2018 software package with AMBER99SB-ILDN force field.[46] The high temperature (500 K) treated Aβ(16-22) were placed at the center of a $9 \times 9 \times 9$ nm^3 box that randomly filled with TIP3P water molecules. The box was neutralized by adding Na^+ counterions if required. The total atom number was 71523 to 74022. The bond lengths of peptides and water molecules were constrained, respectively by the LINCS[47] and SETTLE[48] algorithms, allowing an integration time step of 2 fs. Non-bonded pair lists were updated by every 5 steps. The temperature of all MDs was 310 K. The pressure was kept at 1 bar using the Parrinello–Rahman method[49] with a coupling time constant of 1.0 ps. A cutoff of 1.4 nm was used for van der Waals interactions. The particle mesh Ewald (PME) method[50] with a real space cutoff of 1.0 nm was used for electrostatic interactions. The coordinates were saved every 2 ps. The simulation time in each MD was 600 ns.

Acknowledgment

D.L. gives thanks to Prof. Yunxiang Sun who provided the force field parameters of FG molecule and Prof. Xingfei Zhou who provided AFM facility.

References

[1] Huntley J D and Howard R J 2010 *Int. J. Geriatr. Psychiatry* **25** 121
[2] Morris R G and Mograbi D C 2013 *Cortex* **49** 1553
[3] Gandhi J, Antonelli A C, Afridi A, Vatsia S, Joshi G, Romanov V, Murray I V J and Khan S A 2019 *Rev. Neurosci.* **30** 339
[4] Younkin S G 1998 *J. Physiol.* **92** 289
[5] Citron M 2010 *Nat. Rev. Drug Discov.* **9** 387
[6] Mattson M P 2004 *Nature* **430** 631
[7] Selkoe D J 2001 *Physiol. Rev.* **81** 741
[8] Damante C A, Ösz K, Nagy Z, Grasso G, Pappalardo G, Rizzarelli E and Sóvágó I 2011 *Inorg. Chem.* **50** 5342
[9] Li J, Liu R, Lam K S, Jin L W and Duan Y 2011 *Biophys. J.* **100** 1076
[10] Chimon S, Shaibat M A, Jones C R, Calero D C, Aizezi B and Ishii Y 2008 *Nat. Struct. Mol. Biol.* **14** 1157
[11] Klimov D K and Thirumalai D 2003 *Structure.* **11** 295
[12] Lynn D and Meredith S 2000 *J. Struct. Biol.* **130** 153
[13] Liang C, Ni R, Smith J E, Childers W S, Mehta A K and Lynn D G 2014 *J. Am. Chem. Soc.* **136** 15146
[14] Balbach J J, Ishii Y, Antzutkin O N, Leapman R D, Rizzo N W, Dyda F, Reed J and Tycko R 2000 *Biochemistry* **39** 13748
[15] Dai B, Li D, Xi W, Luo F, Zhang X, Zou M, Cao M, Hu J, Wang W, Wei G, Zhang Y and Liu C 2015 *Proc. Natl. Acad. Sci. USA* **112** 2996
[16] Chen J, Zhu E, Liu J, Zhang S, Lin Z, Duan X, Heinz H, Huang Y and De Yoreo J J 2018 *Science* **362** 1135
[17] Li H, Luo Y, Derreumaux P and Wei G 2011 *Biophys J.* **101** 2267
[18] Lin D, Lei J, Li S, Zhou X, Wei G and Yang X 2020 *J. Phys. Chem. B* **124** 3459
[19] Xie L, Luo Y, Lin D, Xi W, Yang X and Wei G 2014 *Nanoscale* **6** 9752
[20] Li S, Wang L, Chusuei C, Suarez V, Blackwelder P, Micic M, Orbulescu J and Leblanc R 2015 *Chem. Mater.* **27** 1764
[21] Liu Y, Xu L P, Dai W, Dong H, Wen Y and Zhang X 2015 *Nanoscale* **7** 19060
[22] Ngo S T, Truong D T, Tam N M and Nguyen M T 2017 *J. Mol. Graph. Model.* **76** 1
[23] Nespovitaya N, Mahou P, Laine R F, Schierle G S K and Kaminski C F 2017 *Chem. Commun. (Camb).* **53** 1273
[24] Sun Y, Xi W and Wei G. 2015 *J Phys Chem B.* **119** 2786
[25] Bieschke J, Herbst M, Wiglenda T, Friedrich R P, Boeddrich A, Schiele F, Kleckers D, Lopez del Amo JM, Grüning B A, Wang Q, Schmidt M R, Lurz R, Anwyl R, Schnoegl S, Fändrich M, Frank R F, Reif B, Günther S, Walsh D M and Wanker E E 2011 *Nat. Chem. Biol.* **8** 93
[26] Meng F, Abedini A, Plesner A, Middleton C T, Potter K J, Zanni M T, Verchere C B and Raleigh D P 2010 *J. Mol. Biol.* **400** 555

[27] Yang F, Lim G P, Begum A N, Ubeda O J, Simmons M R, Ambegaokar S S, Chen P P, Kayed R, Glabe C G, Frautschy S A and Cole G M 2005 *J. Biol. Chem.* **280** 5892
[28] Necula M, Breydo L, Milton S, Kayed R, van der Veer W E, Tone P and Glabe C G 2007 *Biochemistry* **46** 8850
[29] Lorenzo A and Yankner B A 1994 *Proc. Natl. Acad. Sci. USA* **91** 12243
[30] How S C, Yang S M, Hsin A, Tseng C P, Hsueh S S, Lin M S, Chen R P, Chou W L and Wang S S 2016 *Food Funct.* **7** 4898
[31] Young L M, Saunders J C, Mahood RA, Revill C H, Foster R J, Tu L H, Raleigh D P, Radford S E and Ashcroft A E 2015 *Nat. Chem.* **7** 73
[32] Liu F, Wang W, Xuan Z, Jiang L, Chen B, Dong Q, Zhao F, Cui W, Li L and Lu F 2021 *Int. J. Biol. Macromol.* **170** 33
[33] Lin D, Luo Y, Wu S, Ma Q, Wei G and Yang X 2014 *Langmuir* **30** 3170
[34] Wen G, Qin W, Chen D, Wang Y, Yue X, Liu Z, Cao Y, Du J, Zhou B and Bu X 2017 *Chem. Commun. (Camb).* **53** 3886
[35] Zhang J, Zhou L, Du Q, Shen Z, Hu J and Zhang Y 2019 *Nanoscale.* **11** 8210
[36] Dai B, Kang S G, Huynh T, Lei H, Castelli M, Hu J, Zhang Y and Zhou R 2013 *Proc. Natl. Acad. Sci. USA* **110** 8543
[37] Sedin D L and Rowlen K L 2000 *Anal. Chem.* **72** 2183
[38] Jiang T and Zhu Y. 2015 *Nanoscale* **7** 10760
[39] Kreis C T, Grangier A and Bäumchen O 2019 *Soft Matter* **15** 3027
[40] Sarroukh R, Goormaghtigh E, Ruysschaert J M and Raussens V 2013 *Biochim. Biophys. Acta* **1828** 2328
[41] Kong J and Yu S 2007 *Acta Biochim. Biophys. Sin. (Shanghai).* **39** 549
[42] Kinoshita M, Lin Y, Dai I, Okumura M, Markova N, Ladbury JE, Sterpone F and Lee Y H 2018 *Chem. Commun. (Camb).* **54** 7995
[43] Seong S H, Paudel P, Jung H A and Choi J S 2019 *Mar. Drugs* **17** 600
[44] Lin D, Luo Y, Wu S, Ma Q, Wei G and Yang X 2014 *Langmuir* **30** 3170
[45] Sun Q, Liu F, Sang J, Lin M, Ma J, Xiao X, Yan S, Naman CB, Wang N, He S, Yan X, Cui W and Liang H 2019 *Mar. Drugs* **17** 121
[46] Lindorff-Larsen K, Piana S, Palmo K, Maragakis P, Klepeis J L, Dror R O and Shaw D E 2010 *Proteins* **78** 1950
[47] Hess B, Bekker H, Berendsen H J C and Fraaije J G E M 1997 *J. Comput. Chem.* **18** 1463
[48] Miyamoto S and Kollman P A 1992 *J. Comput. Chem.* **13** 952
[49] Parrinello M and Rahman A 1981 *J. Appl. Phys.* **52** 7182
[50] Darden T, York D and Pedersen L 1993 *J. Chem. Phys.* **98** 10089